Civil and Environmental Research, Vol.5 2013
Special Issue for International Congress on Materials & Structural Stability, Rabat, Morocco, 27-30 November 2013

Can we detect internal moisture content in hardened concrete with an infrared camera?

J. Tápia[1], I. Rodríguez-Abad[1] and R. Martínez-Sala[1]
[1]Universitat Politècnica de València, Camino de Vera s/n, 46012, Valencia, Spain
Corresponding e-mail: isrodab@upvnet.upv.es

Abstract. The main goal of this paper was to assess the ability of infrared thermography to detect non-superficial moisture content in concrete elements. For this purpose, a commercial camera (Flir i5) was used and firstly its capacities and technical limitations were analyzed by comparing it with other commonly commercialized. Secondly, the experiments were undertaken using a concrete specimen (water/cement=0.5) and water under a pressure of 500 kPa was injected over 72 hours into one side of the specimen. The specimen was then left at room temperature (20 ºC) for 24 hours, so the surface moisture disappeared. Prior to the images acquisition, the specimen surface was heated by a lamp located at a distance of 0.68 m from the central point of the specimen. In this way, two areas (dry and injected) to be registered would receive the same energy, since they were equidistant from the heating source. The first record was acquired before heating the specimen and then, the heating process was interrupted every 10 minutes to perform the infrared images acquisitions. Finally, by means of the destructive test, the average water penetration depth was assessed to be 3 cm. The infrared images acquired before heating the specimen showed a small temperature variation as a result of the presence of water, 16,3 ºC in the dry area and 15,8 ºC in the injected area. However, after the heating, due to the greater specific heat of water, the injected part achieved a temperature 4 ºC lower than the symmetrical dry area. This result was very interesting because, in the initial moment (before heating) the surface specimen was dry, but there was a wet area inside of the specimen that was not visually identifiable. Nevertheless, by means of infrared imaging an indicator was obtained that allowed to detect the presence of this internal moisture content.

1 Introduction

Infrared thermography is a non-destructive technique that measures the temperature distribution at the surface of objects. The internal anomalies of those objects can be detected by analyzing the temperature distribution of their surface. An infrared imaging system (an infrared camera) collects the flow of energy, infrared electromagnetic radiation, emitted by a target surface and transforms this energy initially into an electric signal and then into a digital image, called thermogram. Afterwards, with the use of specific software, the surface temperature of objects captured by the camera can be determined.

In inspection terms, this type of instrument has certain advantages, since it does not inflict any damage upon the studied material. The inspection is very quick compared to other techniques, and the results are relatively easy to interpret. Another important aspect of thermography is this technology's great capacity for detecting anomalies produced by the effects of water.

Although thermography is associated with a wide range of applications, when this technique is applied, limits such as the following should be taken into account: depth of detection, minimum resolution of the camera and the subsurface anomalies most easily located, as described in [1] and [2]. To be aware of these limits helps to limit excessive skepticism as well as excessive enthusiasm for thermography as a method of inspection of building materials, and its application on site.

The objective of this work is therefore double. On one hand, to define which are the most important parameters to be considered when using an infrared camera, such as the Flir i5; and on the other, to assess if it is possible to apply infrared thermography to detect internal moisture content in concrete elements.

For this purpose, this research began analyzing the technical characteristics of different infrared cameras. The first step was to evaluate the limits and capacities of the different cameras usually commercialized. A comparison was performed between/among them, in which the most important camera specifications were taken into account.

With the above, and considering the results of authors studying similar concepts [3-7], the experimental program was developed. Firstly, a concrete specimen was fabricated, in which in one part of it water was injected under pressure. Secondly, the specimen was heated and infrared images were acquired from the dry and the injected areas using a Flir i5 camera. Finally, by means of the destructive test, it was possible to assess the average water penetration depth (3 cm).

2 Experimental Program

The first part consisted of an analysis of the technical qualities of the infrared cameras available on the market. With this purpose, 16 cameras were chosen to be evaluated from the 4 commercial brands most used currently.

For the second part of the study, a concrete specimen was fabricated, which dimensions are 60 x 20 x 7.5 cm. The water/cement ratio was 0.5 and the mixture proportions were as follows: CEM I 360 kg/m³, water 180 kg/m³, sand 1238 kg/m³ and gravel 694 kg/m³. Water under a pressure of 500 kPa was injected over 72 hours into one side of the specimen, following the procedure established under the standard UNE-EN 12390-8 [8]. The specimen was then left at room temperature (20 ℃) for 24 hours so the surface moisture disappeared. By means of a destructive test we knew that the water had penetrated to a depth of 3cm in a spherical form, as can be seen in figure 1a.

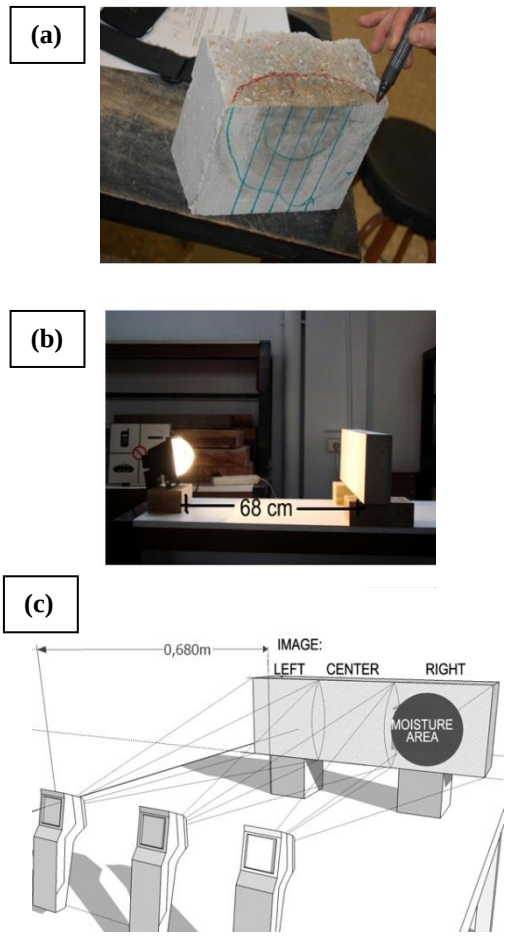

Fig. 1. (a) Concrete specimen with which a destructive test was undertaken to measure the water penetration depth; (b) Distance between the heat source and the concrete specimen; (c) Position of the camera when the images were taken: left, centre and right.

A Flir i5 infrared camera was used to capture the infrared images. Prior to images acquisition, the surface of the specimen was heated by a single 500 W halogen lamp. The lamp was located at a distance of 0.68 m from the central point of the specimen (figure 1b). In this way we could be sure that the 2 areas to be registered would receive the same energy, since they were equidistant from the heating source. The first image was recorded in the initial conditions (24 hours after the injection of water), and after that, the heating process was started. Subsequently, the heating process was interrupted every 10 minutes to perform infrared images acquisitions.

In every record session, three images of the specimen surface were acquired: two on the extremes (right and left) and one central. As it is shown in figure 1c, the three images covered completely the concrete surface. During the sessions the laboratory environmental conditions were controlled, specifically humidity (RH= 60%) and temperature (20 ℃), to ensure that all images were recorded in the same conditions.

Use a two-column format, and set the spacing between the columns at 8 mm. Insert short form title of the conference “CMSS-2013” in headers, except the first one. Do not add any page numbers.

3 Results

3.1 Evaluation of camera qualities

The most significant parameter values of the 16 cameras studied in this work are detailed in table 1.

Table 1. The most significant characteristics of 16 infrared cameras.

Camera	Minimum distance (m)	Thermal sensitivity (℃)	IR Resolution (pixel)	Spatial resolution (mrad)
Flir i5	**0,60**	**0,10**	**6.400**	**3,71**
Flir i7	0,60	0,10	14.400	3,71
Flir B40	0,10	0,10	14.400	3,64
Flir B50	0,10	0,09	19.600	3,12
Flir B60	0,10	0,07	32.400	2,42
Flir B250	0,40	0,07	43.200	2,18
Flir B365	0,40	0,05	76.800	1,36
Flir B425	0,40	0,03	76.800	1,36
Flir B620	0,30	0,04	307.200	0,65
Flir B660	0,30	0,03	307.200	0,65
Fluke TiRx	0,15	0,10	19.200	2,50
Fluke TiR	0,15	0,10	19.200	2,50
Fluke TiR1	0,15	0,07	19.200	2,50
Fluke TiR32	0,45	0,05	76.800	2,50
NEC F30S	0,10	0,10	19.200	3,10
ICI-toughcamP	0,10	0,06	19.200	1,90

From the analysis of the values in table 1 it can be observed that:

Minimum distance. This refers to the minimum distance necessary between the camera and the object to be analysed to obtain a good quality image. In the case of the cameras analysed, this

distance was between 0.10 and 0.60 m. The Flir i5 has a minimum distance of 0.60 m.

Thermal sensitivity**.** The majority of the cameras detect a difference of 0,1 ℃, and the most sensitive models (Flir B 425 and 660) detect a difference of 0,03 ℃.

IR Resolution**.** The difference in resolution between the models Flir B 620 and 660 (640 x 480 pixels, 307200 pixels per image) and the rest was significant as it can be observed in table 1. The camera with the lowest resolution is the Flir i5, with a total of 6400 pixels.

Spatial resolution**.** This is the angle covered by each pixel of the sensor. The best image quality is provided by those cameras with a spatial resolution of 0.65 mrad (Flir B 620 and 660). Most cameras have a spatial resolution of approximately 3 mrad, and the higher value is presented by the Flir i5 with 3.71 mrad.

There are two cameras (Flir B 620 and 660) which, due to their advantages, are significantly superior to the other cameras available. The same brand produces the camera with the weakest profile, the Flir i5, which is the one used in this experiment. However, if the infrared images are acquired at a distance of 0.60 m the resulting images could achieve enough definition, since the size of the pixel at 0,60 m is 0,76 x 0,76 cm, providing a total of 576 pixels per image. This resolution is more than enough when analyzing temperature differences on the surface of concrete.

3.2 Analysis of the infrared images

To analyze the results, three distinctive areas of the specimen were recognized: the area where the water was injected (right), the area adjacent to this (central) and the opposite side, furthest from the moisture (left).

Before the application of the heat source, the temperature of these three areas was very similar (figure 2). Their colour was homogeneous, indicating that the temperature was approximately uniform. However, 70 minutes after the application of the heat source, the temperature distribution over the surface was not homogeneous. As it was expected, the area, in which the heating source was closest, achieved the highest temperature (the lightest yellow area in the central image of figure 3). It can also be observed that in the right and left images the temperature increased at different rates (ΔT_{right}=6.1 ℃ and ΔT_{left}=9.6 ℃).

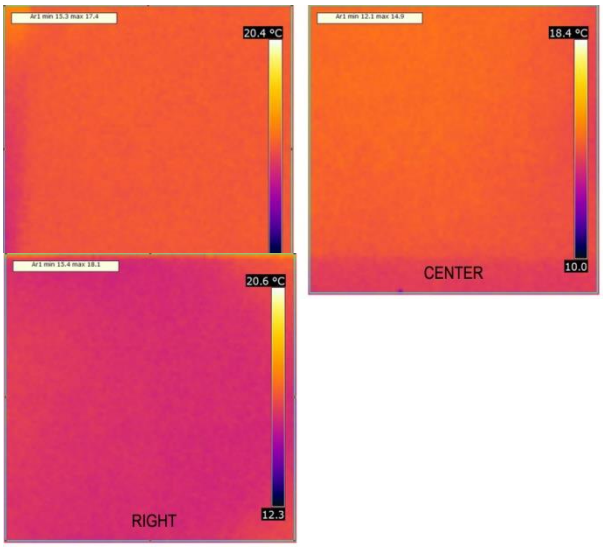

Fig. 2. Left, central and right areas thermograms of the specimen recorded in the initial state, before heating.

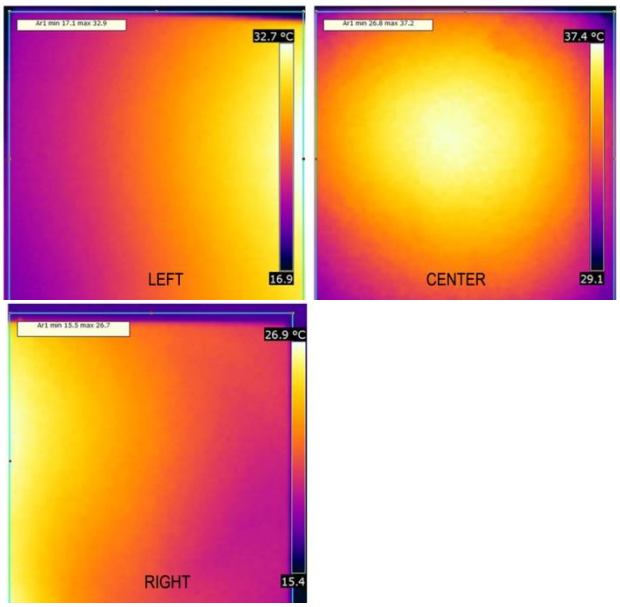

Fig. 3. Left, central and right areas thermograms of the specimen recorded after heating it for 70 minutes.

The average temperature of every infrared image was calculated and plotted in function of time (figure 4). As it can be observed, the specimen showed a small temperature variation as a result of the presence of water, in the infrared images recorded before heating. The initial temperatures were 14 ℃ in the central area, 16.3 ºC in the dry one (left) and 15.8 ℃ in the injected one (right). After the application of the heat source over 70 minutes, the temperature in the central image increased up to 34 ℃, in the left image up to 25.9 ℃ and in the right one up to 21.9 ℃.

This means that for the same quantity of applied energy, the injected part of the specimen achieved a temperature 4 ℃ lower than the symmetrical dry area. This was due to the greater specific heat of water.

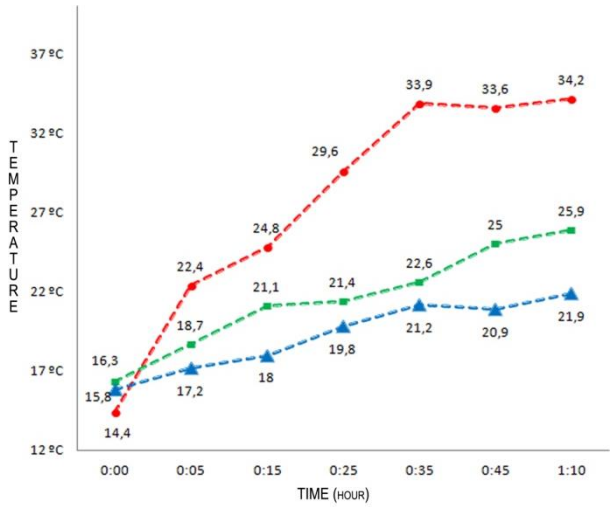

Fig. 4. Graph showing temperature change in the 3 areas of the concrete specimens. The red dashed line represents the temperature increase in the central image, the green one the increase in the dry zone (left image) and the blue one the increase in the moisturized area (right image).

4 Conclusions

Regarding the analysis of the principal characteristics of infrared cameras, it is important to highlight that, depending on the purpose of the study, superior and inferior cameras do not exist. What it is necessary to know is if technical characteristics of each unit provide enough resolution for the target under study.

Nevertheless, image resolution and corresponding colour assignation is very limited with the Flir i5. However, this limitation can be compensated through digital manipulation of the image with specific software.

In relation to the conducted experiment, it was proved that internal moisture content, close to the surface of a concrete specimen (approximately 3 cm), could be detected by means of infrared thermography; even if this internal moisture content was not visually noticeable on the surface.

Before applying a heat source, the temperature difference was only 0.5 ºC between the dry and the injected area. But, results showed that after an equal amount of heating was applied to two different areas of the specimen, one completely dry and the other where water was injected, always lower temperatures were observed in the images corresponding to that part of the specimen in which water was injected. Indeed, after 70 minutes of heating, temperature differences of 4 ºC were detected experimentally between them.

References

1. D. González Fernández, Contribuciones a las técnicas no destructivas para evaluación y prueba de procesos y materiales basadas en radiaciones infrarrojas. PhD Thesis, Universidad de Cantabria, Spain, (2006)
2. E. Gayo Moncó, La humedad como causa de patologías monumentos: desarrollo de nuevas técnicas análisis no destructivo basadas termografía infrarroja, PhD Thesis, Universidad Complutense de Madrid, Spain, (1999).
3. Caleb Hing, B. Udaya, Halabe, Nondestructive testing of GFRP bridge decks using ground-penetrating radar and infrared thermography, Journal of Bridge Engineering, **15,** 391-398, (2010).
4. Ch. Maierhofer, A. Brink, M. Reollig, H. Wiggenhauser, Transient thermography for structural investigation of concrete and composites in the near surface region. Infrared Physics & Technology, **43**, 271–278, (2002).
5. Ch. Maierhofer, R. Arndt, R. Rollig, Influence of concrete properties on the detection of voids with impulse-thermography, Infrared Physics & Technology, **49**, 213–217, (2007).
6. Chia-Chi Cheng, Tao-Ming Cheng, Chih-Hung Chiang, Defect detection of concrete structures using both infrared thermography and elastic waves, Automation in Construction, **18**, 87 – 92, 2008.
7. E. Barreira, V. de Freitas, Evaluation of building materials using infrared thermography, Construction and building materials, **21**, 218-224, 2007.
8. UNE-EN 12390-8 “Testing hardened concrete”, Part 8: Depth of penetration of water under pressure.